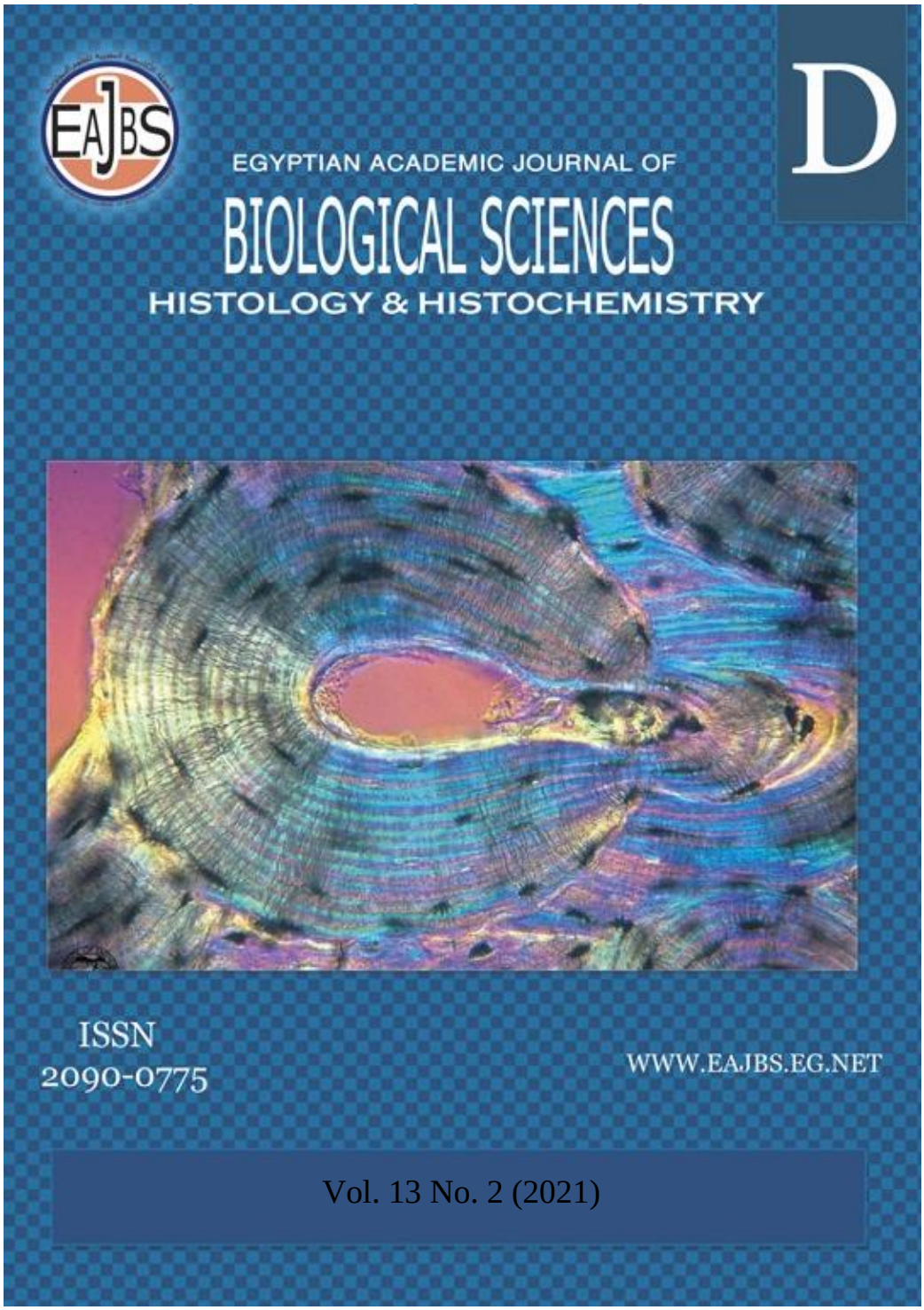

Citation: Egypt. *Acad. J. Biolog. Sci. (D-Histology and histochemistry) Vol.13(2) pp135-150(2021)*
DOI: 10.21608/EAJBSD.2021.210041

Egypt. Acad. J. Biolog. Sci., 13(2): 135-150 (2021)

Egyptian Academic Journal of Biological Sciences
D. Histology & Histochemistry
ISSN 2090 – 0775
http://eajbsd.journals.ekb.eg

Effects of Nicotine and Its Withdrawal on The Postnatal Development of Rat Mitral Cells

Ayman S. Amer* and Dorreia A.M. Zaghloul
Department of Human Anatomy and Embryology, Faculty of Medicine, Assiut University, Assiut, Egypt
E.Mail: ayman.amer@aun.edu.eg

ARTICLE INFO
Article History
Received:30/11/2021
Accepted:21/12/2021

***Keywords*:**
Nicotine, Postnatal development, Olfactory bulb, Mitral cells ultrastructure

ABSTRACT

Background: Cigarette smoking is a public health problem worldwide. Nicotine content in cigarettes causes dependence and many diseases. Olfactory bulb neurons are damaged early in neurodegenerative diseases. **Aim of the work:** to demonstrate effects of nicotine administration on the structure of mitral cells of olfactory bulbs in growing rats, and the outcome of nicotine withdrawal. **Materials and Methods:** 24 pregnant rats were randomly equally divided into two groups; a control group received no treatment, and a treated group received nicotine 6 mg/kg body weight/day subcutaneously daily from gestational day 8 until postnatal day 21. Six male offspring rats in each group at ages of newborn, 10 days, 21 days, and 2 months were included in this study. On the postnatal day 21, six male offspring rats were sacrificed, and another six rats were allowed to survive without any treatment until the age of 2 months and considered as the recovery group. Olfactory bulbs were dissected, fixed, and processed for light and transmission electron microscopy. **Results:** olfactory bulbs in all ages of the treated group had neuropil vacuolations in several layers. Mitral cells were degenerating with shrunken nuclei, nuclear membrane indentations, cytoplasmic and mitochondrial vacuolization, and lipofuscin granules as compared to the control. Neurodegenerative changes increased with increasing the age of rats and showed widened perinuclear spaces and swollen irregular axons with splitting of myelin sheaths at postnatal day 21 as compared to the control. Upon nicotine withdrawal, the structure of olfactory bulbs returned to normal features. **Conclusion:** Nicotine induced neurodegenerative changes in mitral cells. Recovery of mitral cells to normal occurred upon nicotine withdrawal.

INTRODUCTION

Cigarette smoking is considered the most prevalent type of substance dependence, causing serious public health-related problems worldwide. Nicotine is the main chemical substance in cigarettes with cognitive-enhancing effects that make it hard to quit smoking (Valentine and Sofuoglu, 2018; Fowler *et al.*, 2020). Many brain imaging reports have shown activation of the brain centers responsible for attention and working memory performance after nicotine exposure (Rose *et al.*, 2003). Nicotine also acts as an agonist in presynaptic nicotinic acetylcholine receptors, thus facilitating the synaptic release of several neurotransmitters (Singer *et al.*, 2004).

These receptors are involved in the regulation of nicotine rewarding properties, development of nicotine dependence, and effects of its withdrawal (Fowler *et al.,* 2008). On the other hand, previous researchers reported the cytotoxic effects of nicotine, and that maternal exposure to nicotine leads to several deleterious effects in the fetus (Wong *et al.*, 2015). Nicotine also accumulates in breast milk, thus leading to significant tissue damage in the suckling pups (Wong *et al.*, 2015). Furthermore, the exposure to nicotine during pregnancy carries significant risks including fetal growth retardation, preterm rupture of membranes and increased perinatal mortality (Nemati *et al.*, 2021).

Olfaction is one of the special senses that are jeopardized by exposure to neurotoxic chemicals. The olfactory bulb is the first relay center of olfactory information in the mammalian central nervous system (Imamura *et al*., 2020). In the olfactory bulb, axons of the olfactory nerve form synapses with dendrites of projection neurons that transmit the olfactory information to the olfactory cortex. The olfactory neurons are capable of neurogenesis (Kouremenou *et al.*, 2020; Durante *et al.*, 2020). Olfactory bulb projection neurons have been classified into two populations, mitral cells and tufted cells. The size of mitral cell somata (20–25 mm) is much larger than that of tufted cells (10–20 mm). Cell bodies of these neurons are located within specific layers of the olfactory bulb; the mitral cells are in the mitral cell layer (a single-cell layer) while the tufted cells are found in the external plexiform layer (Imamura *et al.*, 2020).

Many *in vivo* and *in vitro* studies postulated that nicotine might be neuroprotective for neuronal populations submitted to toxic or ischemic insults (Chambers *et al.*, 2013; Iwamoto *et al.*, 2013; Yang *et al.*, 2019). However, several previous studies have highlighted the brain-damaging properties of nicotine in different cerebral regions (Chen *et al.*, 2003). To our knowledge, the structural and ultrastructural effects of nicotine and its withdrawal on the olfactory mitral cells were scantly studied before.

Therefore, the current study is designed to demonstrate the effects of nicotine administration during pregnancy and lactation on the structure of the mitral cells of the olfactory bulb in the growing rats. We also investigated whether the withdrawal of nicotine would change the outcome or not?

MATERIALS AND METHODS

Chemicals:

Nicotine: Synonyms 3-(1-Methyl-2-pyrrolidinyl) pyridine, (S)-(-)-Nicotine 100% concentration (Cat. No. 109535, Product number: 8208770025, glass bottle (25 ml) was obtained from Merck KGaA Frankfurter Str. 250, 64293 Darmstadt Germany.

Animals:

A total of 24 healthy adult females (3 months aged weighing 180-200 gm), and 12 adult males (3 months aged weighing 200-250 gm) albino rats were obtained from the animal house, Faculty of Medicine, Assiut University, Assiut, Egypt. Rats were kept in metal cages under controlled room temperature with a 12 h light/dark cycle during the research period. Food (standard rat chow) and water were available ad libitum. This experimental study was fully approved by the Local Ethical Committee and by the Institutional Review Board of Faculty of Medicine, Assiut University and was carried out in accordance with relevant guidelines and regulations of the Animal Care Guidelines of the National Institutes of Health. The experimental procedures affirm that all animals received humane care and appropriate measures were taken to minimize animal pain or discomfort.

Experimental Design:

The female rats were mated with males overnight, and the presence of a

vaginal plug that contains sperms was recorded as gestational day zero. 24 pregnant rats were singly housed, and randomly and equally divided into two groups; a control group received no treatment, and a treated group received nicotine (6 mg/kg body weight/day, subcutaneously, dissolved in normal saline) from the gestational day 8 through parturition and lactation until weaning at postnatal day 21. The administration of this dose in rats simulated the plasma nicotine levels found in heavy smokers (Matta *et al.*, 2007). Six male offspring rats from each group were included in this study at the ages of newborn, 10 days, 21 days, and 2 months. On the postnatal day 21, the six male offspring rats were sacrificed, and another six male offspring rats were allowed to survive without any treatment until the age of 2 months and were considered as the recovery group. The research period continued until the offspring's age of 2 months. Rats were anaesthetized by ether inhalation and subjected to intracardiac perfusion of normal saline 0.9% Na Cl into the left ventricle, then euthanized by cervical dislocation for tissue specimen collection. Brain specimens were extracted from the rats, and the olfactory bulb was dissected, and coronal sections were made at the mid-point of olfactory bulbs for histological studies.

Light Microscopic Study:

Six olfactory bulb specimens from each age group were fixed in 10% neutral-buffered formalin, dehydrated, and then cleared in xylene and embedded in paraffin. 5-micron thick serial sections were prepared. The sections were stained with Hematoxylin & Eosin stain according to a previous protocol (Suvarna *et al.*, 2019). Randomly selected stained slides were examined with an Olympus CX41 microscope, and photos were taken by an Olympus DP72 CCD digital camera (Olympus Corporation, Tokyo, Japan) attached to the microscope at the Human Anatomy and Embryology Department, Faculty of Medicine, Assiut University, Egypt.

Electron Microscopic Study:

Olfactory bulb specimens of six rats from each age group were fixed in 2.5% glutaraldehyde in sodium cacodylate buffer at pH 1.5 for 24 hours and then post-fixed in 1% osmium tetroxide for one hour (Kuo, 2014). The fixative was then washed out by distilled water and dehydration series were done. The specimens were embedded in fresh resin and incubated overnight at 60ºC. Semithin sections (one-micron thickness) were cut, stained with toluidine blue, and examined by light microscopy. Ultrathin sections (450–500 Aº) from selected areas were contrasted and stained with an alcoholic solution of uranyl acetate followed by aqueous lead citrate (Kuo, 2014), examined, and photographed by the transmission electron microscope (TEM) (JEOL Ltd. E.M.-100 CX11; Tokyo, Japan) at the Assiut University Electron Microscopy Unit, Egypt.

RESULTS

Effects of Nicotine on The Histopathological Features of Olfactory Bulbs of Newborn Rats:

The histological examination of the olfactory bulbs in the newborn control group shows the normal cytoarchitecture which is formed of six layers of the olfactory bulb from superficial to deep: olfactory nerve layer (ONL), glomerular layer (GL), external plexiform layer (EPL), mitral cell layer (MCL), internal plexiform layer (IPL), and granular cell layer (GCL) (Fig. 1A). The semithin sections show the mitral cells somata as a single row located within the MCL. Mitral cells have abundant cytoplasm and lightly stained basophilic vesicular nuclei with prominent nucleoli (Fig. 1B). In addition, numerous granule cells somata make up most of the cells in the MCL. The transmission electron microscopy shows healthy mitral cells with rounded euchromatic nuclei. The surrounding cytoplasm is rich in

organelles and has many mitochondria, free ribosomes, and rough endoplasmic reticulum (Fig. 1C).

In the newborn-treated group, the olfactory bulbs show widened intercellular spaces and vacuolations are present in the neuropil of the ONL and EPL (Fig. 2A). Semithin sections reveal the MCL containing mitral cells with large vesicular nuclei and prominent nucleoli. The intercellular spaces appear widened compared to the control group. Some mitral cells are degenerating and appear very lightly stained (Fig. 2B). Using the transmission electron microscope indicates the presence of degenerating mitral cells with irregular electron-dense nuclei and many indentations at the nuclear membrane. The surrounding cytoplasm is rarified and has a few organelles, damaged and vacuolated mitochondria, and lipofuscin granules that make agglomerations. Many vacuolations appear in the cytoplasm of the mitral cells, and lysosomes are seen, in addition to a few free ribosomes and diminished rough endoplasmic reticulum cisternae (Fig. 2C).

Effects of Nicotine on The Histopathological Features of Olfactory Bulbs of 10-Day-Old Rats:

Light microscopy of the olfactory bulbs in the 10-day-old control group shows a healthy normal appearance of the layers of the olfactory bulb from the superficial olfactory nerve layer (ONL) to the deep granular cell layer (GCL) (Fig. 3A). The toluidine blue-stained semithin sections reveal healthy mitral cells with rich cytoplasm and large lightly stained basophilic nuclei that lie in the mitral cell layer (MCL) (Fig. 3B). Electron microscopic examination of the mitral cells demonstrates rounded euchromatic nuclei, and the surrounding cytoplasm has many mitochondria, free ribosomes, and rough endoplasmic reticulum cisternae (Fig. 3C).

In the 10-day-old treated group, the structure of the olfactory bulbs indicates the presence of many vacuolations, evident in the neuropil of the ONL and GCL (Fig. 4A). Semithin sections show the mitral cells with darkly stained somata, and some of the mitral cells appear shrunken. Vacuolization and increased intercellular spaces are seen in the layers of the olfactory bulb (Fig. 4B). The ultrastructural study of the MCL indicates the presence of markedly damaged mitral cells with shrunken condensed nuclei with indentation of the nuclear membrane. The cytoplasm is rarified with severely destroyed organelles, leaving few damaged mitochondria, and lipofuscin granules that form agglomerations. Many vacuolations appear in the cytoplasm with a few free ribosomes, lysosomes, and scarce rough endoplasmic reticulum (Fig. 4C).

Effects of Nicotine on The Histopathological Features of Olfactory Bulbs Of 21-Day-Old Rats:

Microscopic examination of olfactory bulbs in the 21-day-old control group demonstrates the normal architecture of the layers of the olfactory bulb. There is an apparent increase in the thickness of all layers from the olfactory nerve layer (ONL) to the granular cell layer (GCL) as compared to the newborn control group (Fig. 5A). The mitral cells are healthy and appear as the largest cells seen in the mitral cell layer (MCL) (Fig. 5B). The ultrastructure of the mitral cell reveals a rounded euchromatic nucleus and prominent nucleolus. The surrounding cytoplasm has many mitochondria, plenty of free ribosomes and rough endoplasmic reticulum. Normal axons are seen covered with intact darkly stained myelin sheaths (Fig. 5C).

In the 21-day-old treated group, the olfactory bulbs show many vacuolations in the neuropil of ONL and external plexiform layers (EPL) (Fig. 6A). The degenerating mitral cells are darkly stained and have pyknotic nuclei. Increased intercellular spaces, vacuolations and engorged blood

vessels are also evident in the MCL and GCL (Fig. 6B). Ultrathin sections show damaged mitral cells with shrunken irregular heterochromatic nuclei and widened perinuclear spaces. Cytoplasmic organelles are scanty with marked vacuolization. Vacuolated mitochondria, lysosomes, and lipofuscin granules are observed. Swollen irregular axons are seen with splitting, corrugation, and irregularity of the surrounding myelin sheaths (Fig. 6C).

Effects of Nicotine Withdrawal on The Histopathological Features of Olfactory Bulbs of The Recovery 2-Month-Old Rats:

In the 2-month-old rats of the control group, the histology of the olfactory bulbs shows healthy normal features of its six layers with increased thickness of its layers as compared to the 21-day-old rats (Fig. 7A). Semithin sections reveal well-developed mitral neurons having lightly stained vesicular nuclei located in the mitral cell layer (MCL). The mitral cell axon is covered by a myelin sheath which was lost during preparation leaving an empty space. The axon passes through the internal plexiform layer (IPL) to reach the granular cell layer (GCL). Primary dendrite is also evidently extending in the inner layer of the external plexiform layer (EPL) (Fig. 7B). TEM demonstrates mitral cells with euchromatic nuclei, prominent nucleoli, and rich cytoplasm containing many mitochondria, free ribosomes, and rough endoplasmic reticulum (Fig. 7C).

In the recovery 2-month-old rats, the microscopic findings indicate a return to the normal histology of the olfactory bulb. A healthy appearance of the 6 layers of the olfactory bulb is observed (Fig. 8A). However, a very few of the mitral cells are small-sized and darkly stained (Fig. 8B). The ultrastructural study indicates normal mitral cells with oval euchromatic nuclei, peripheral heterochromatin, and abundant cytoplasm rich in many healthy organelles (Fig. 8C).

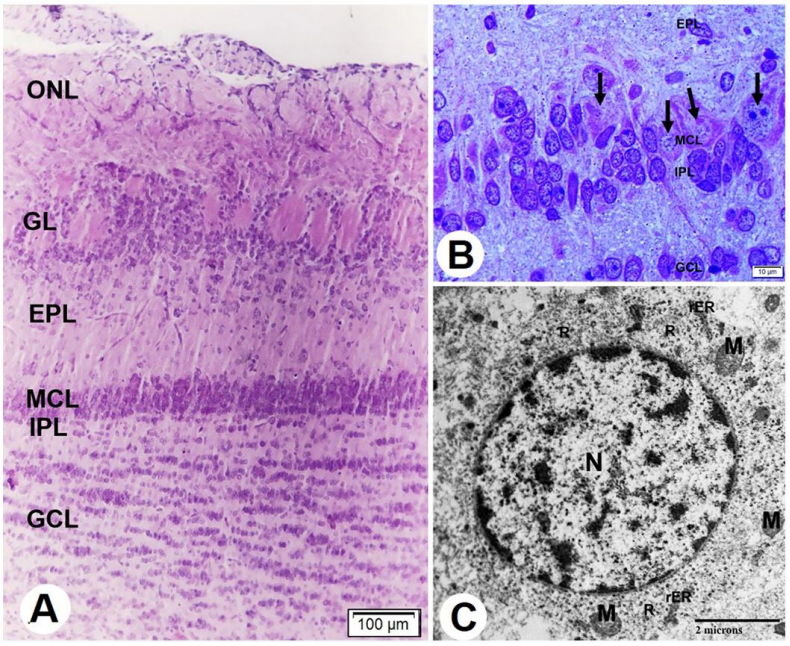

Fig. 1 [A-C]: Photomicrographs of rats' olfactory bulb sections of newborn control group. **[A]:** Showing layers of the olfactory bulb, from superficial to deep: olfactory nerve layer (ONL), glomerular layer (GL), external plexiform layer (EPL), mitral cell layer (MCL), internal plexiform layer (IPL), and granular cell layer (GCL). (H&E, ×100). **[B]**: A semithin section showing the mitral cells (arrows) having abundant cytoplasm and large lightly stained vesicular nuclei with prominent nucleoli located in the MCL. (Toluidine blue, ×1000). **[C]:** A transmission electron micrograph showing a mitral cell with rounded euchromatic nucleus (N). The surrounding cytoplasm has many mitochondria (M), free ribosomes (R) and rough endoplasmic reticulum (rER). (Uranyl acetate and Lead citrate, ×10000).

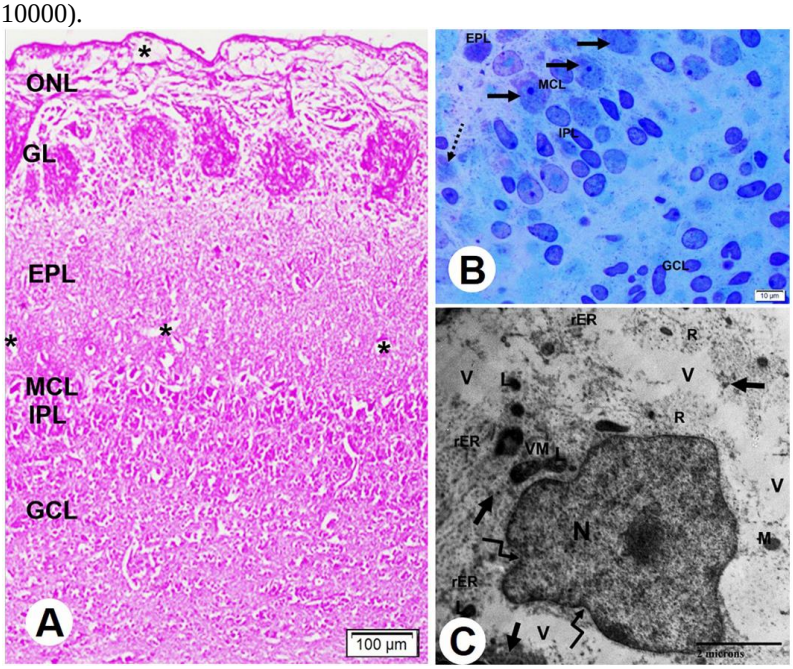

Fig. 2 [A-C]: Photomicrographs of rats' olfactory bulb sections of newborn treated group. **[A]:** Showing layers of the olfactory bulb, from superficial to deep: olfactory nerve layer (ONL), glomerular layer (GL), external plexiform layer (EPL), mitral cell layer (MCL), internal plexiform layer (IPL), and granular cell layer (GCL). The neuropil shows vacuolar spaces (*) at the ONL and EPL. (H&E, ×100). **[B]:** A semithin section showing the mitral cells (arrows) having large vesicular nuclei with prominent nucleoli located in the MCL. Some mitral cells appear very lightly stained (dotted arrow) (Toluidine blue, ×1000). **[C]:** A transmission electron micrograph showing degenerating mitral cell with irregular electron-dense nucleus (N) and many indentations at the nuclear membrane (indented arrows) are seen. The surrounding cytoplasm has scarcity of organelles, few damaged mitochondria (M), vacuolated mitochondria (VM), and lipofuscin granules (thick arrows) forming agglomerations. Many vacuolations (V) appear in the cytoplasm with lysosomes (L), few free ribosomes (R) and rough endoplasmic reticulum (rER). (Uranyl acetate and Lead citrate, ×10000).

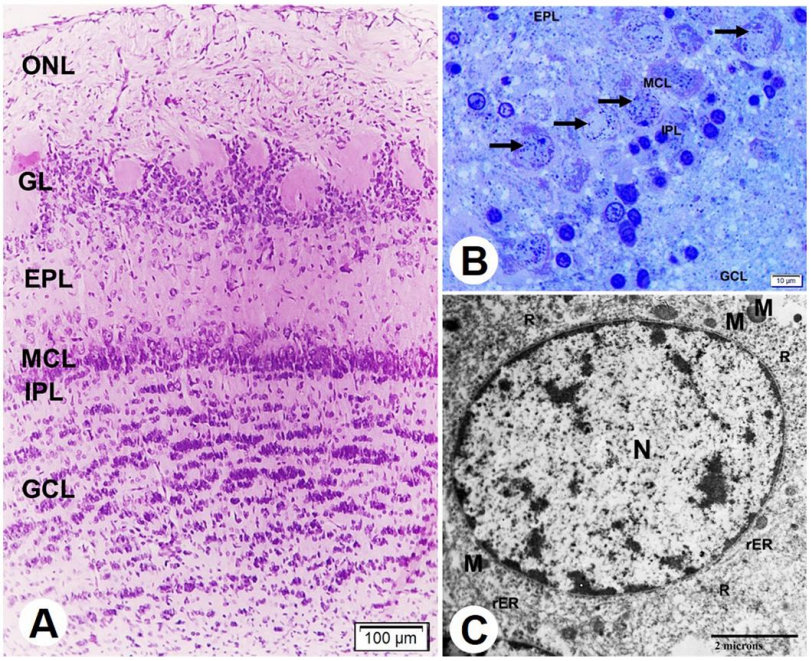

Fig. 3 [A-C]: Photomicrographs of rats' olfactory bulb sections of 10-day-old control group. **[A]:** Showing healthy appearance of the layers of the olfactory bulb. (H&E, ×100). **[B]**: A semithin section showing the mitral cells (arrows) having rich cytoplasm and large lightly stained basophilic vesicular nuclei located in the MCL. (Toluidine blue, ×1000). **[C]:** A transmission electron micrograph showing a mitral cell with rounded euchromatic nucleus (N). The surrounding cytoplasm has many mitochondria (M), free ribosomes (R) and rough endoplasmic reticulum (rER). (Uranyl acetate and Lead citrate, ×10000).

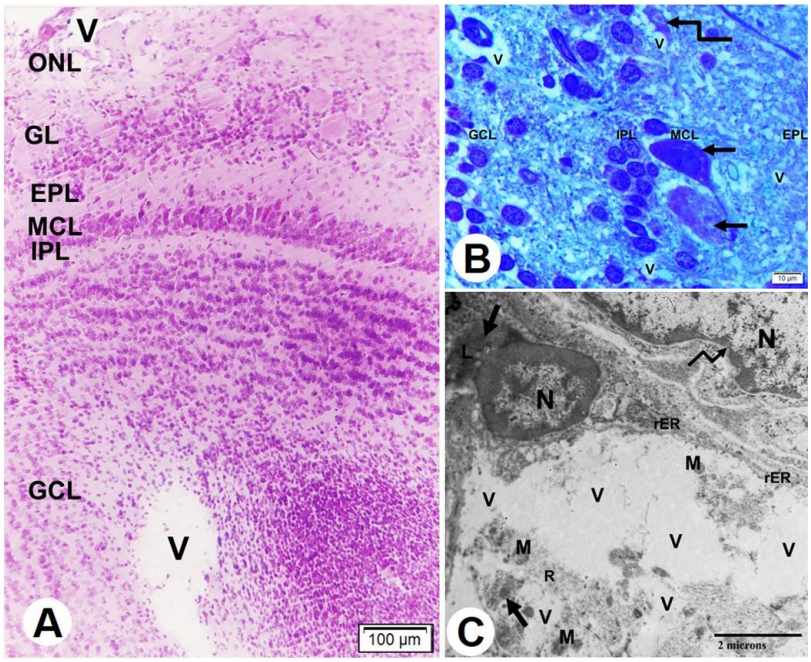

Fig. 4 [A-C]: Photomicrographs of rats' olfactory bulb sections of 10-day-old treated group. **[A]:** Showing the layers of the olfactory bulb. Vacuolations (V) are seen in the neuropil of olfactory nerve layer (ONL) and the granular cell layer (GCL). (H&E, ×100). **[B]:** A semithin section showing the external plexiform layer (EPL), mitral cell layer (MCL), internal plexiform layer (IPL), and granular cell layer (GCL). MCL has darkly stained mitral cells (arrows), and some of the mitral cells appear shrunken (indented arrow). Many vacuolations (V) are seen in the layers of the olfactory bulb. (Toluidine blue, ×1000). **[C]:** A transmission electron micrograph showing a markedly damaged mitral cell has shrunken condensed nucleus (N) with aggregated heterochromatin, and rarified cytoplasm with scarcity of organelles, few damaged mitochondria (M), lipofuscin granules (thick arrows) forming agglomerations. Many vacuolations (V) appear in the cytoplasm with a few free ribosomes (R), lysosomes (L) and rough endoplasmic reticulum (rER). A part of another cell is seen with indentation of the nuclear membrane (indented arrow). (Uranyl acetate and Lead citrate, ×10000).

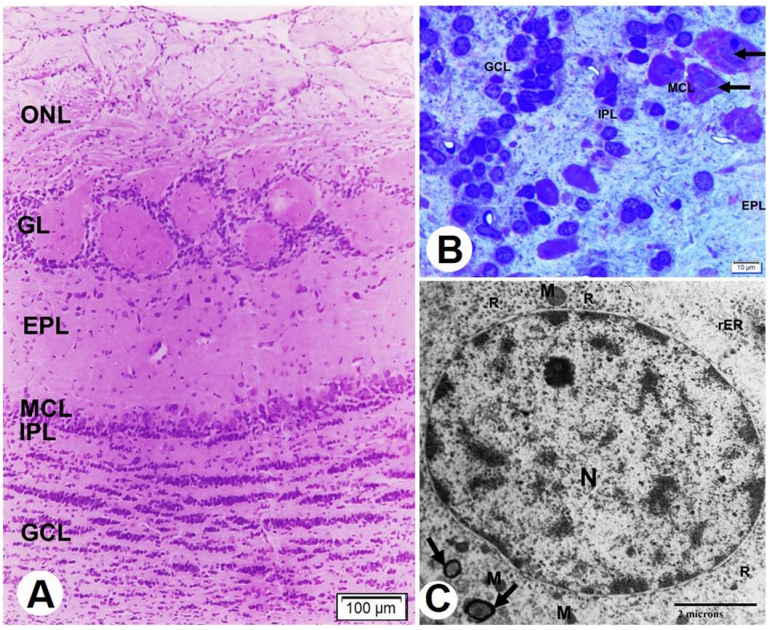

Fig. 5 [A-C]: Photomicrographs of rats' olfactory bulb sections of 21-day-old control group. **[A]:** Showing normal cytoarchitecture of the layers of the olfactory bulb, from the superficial olfactory nerve layer (ONL) to the deep granular cell layer (GCL). (H&E, ×100). **[B]**: A semithin section showing the mitral cells (arrows) having large vesicular nuclei with prominent nucleoli located in the mitral cell layer (MCL). (Toluidine blue, ×1000). **[C]:** A transmission electron micrograph showing a mitral cell with rounded euchromatic nucleus (N) and prominent nucleolus. The surrounding cytoplasm has many mitochondria (M), plenty of free ribosomes (R) and rough endoplasmic reticulum (rER). Axons covered with intact darkly stained myelin sheaths are also seen (thick arrows). (Uranyl acetate and Lead citrate, ×10000).

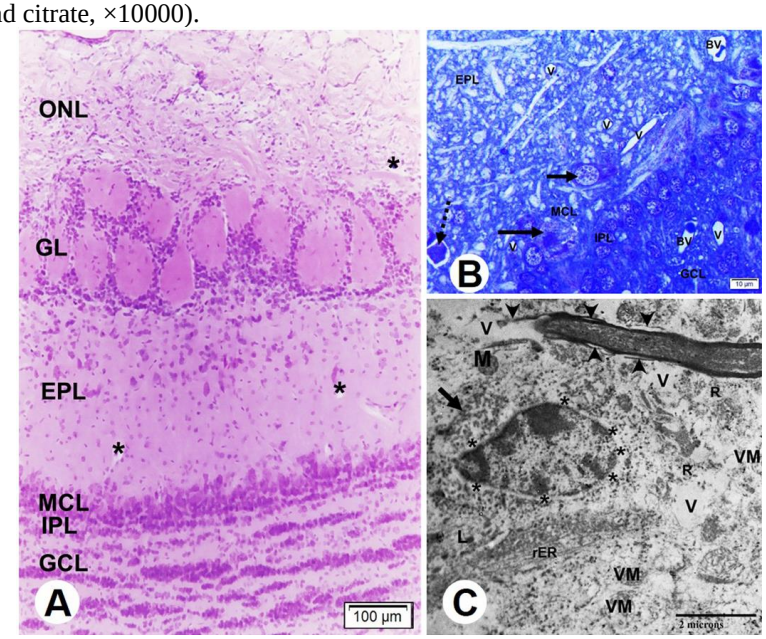

Fig. 6 [A-C]: Photomicrographs of rats' olfactory bulb sections of 21-day-old treated group. **[A]:** Showing the layers of the olfactory bulb. Vacuolar spaces (*) in the neuropil are seen in the olfactory nerve layer (ONL) and the external plexiform layer (EPL). (H&E, ×100). **[B]:** A semithin section showing the EPL, mitral cell layer (MCL), internal plexiform layer (IPL), and granular cell layer (GCL). Mitral cells (arrows) have large vesicular nuclei with prominent nucleoli located in the MCL. Degenerated mitral cells appear darkly stained and pyknotic (dotted arrow). Vacuolations (V) are seen in the EPL, MCL, and GCL layers. Engorged blood vessels (BV) are noticed in the MCL and GCL layers. (Toluidine blue, ×1000). **[C]:** A transmission electron micrograph showing a damaged mitral cell with shrunken irregular heterochromatic nucleus (N) and dilatation of the perinuclear space (*). Few dispersed cytoplasmic organelles are seen; apparent reduction in the number of mitochondria (M), free ribosomes (R), and rough endoplasmic reticulum (rER). Cytoplasmic vacuolization (V) is evident, and vacuolated mitochondria (VM), lysosomes (L), and lipofuscin granules (thick arrow) are present. A swollen irregular axon is seen with splitting, corrugation, and irregularity of the surrounding myelin sheath (arrowheads). (Uranyl acetate and Lead citrate, ×10000).

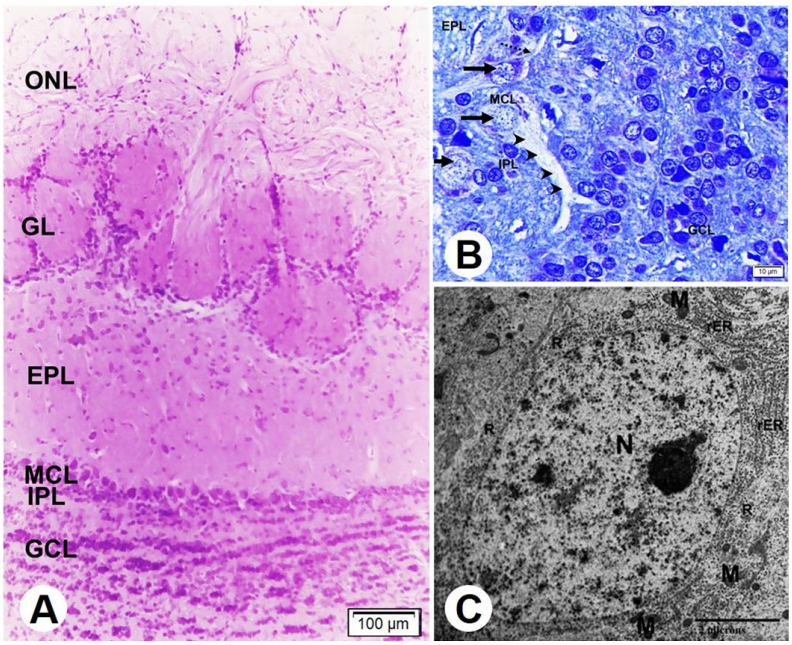

Fig. 7 [A-C]: Photomicrographs of rats' olfactory bulb sections of 2-month-old control group. **[A]:** Showing healthy architecture of the layers of the olfactory bulb, from the superficial olfactory nerve layer (ONL) to the deep granular cell layer (GCL). (H&E, ×100). **[B]:** A semithin section showing the mitral cells (arrows) having abundant cytoplasm and large lightly stained vesicular nuclei located in the mitral cell layer (MCL). The mitral cell has axon and dendrite. The myelin sheath which surrounds the axon was lost during preparation leaving an empty space shown (arrowheads). The axon is seen passing through the internal plexiform layer (IPL) to reach the granular cell layer (GCL). A primary dendrite is also seen (dotted arrow). (Toluidine blue, ×1000). **[C]:** A transmission electron micrograph showing the mitral cell with euchromatic nucleus (N) and prominent nucleolus. The surrounding cytoplasm has many mitochondria (M), free ribosomes (R) and rich rough endoplasmic reticulum (rER). (Uranyl acetate and Lead citrate, ×10000).

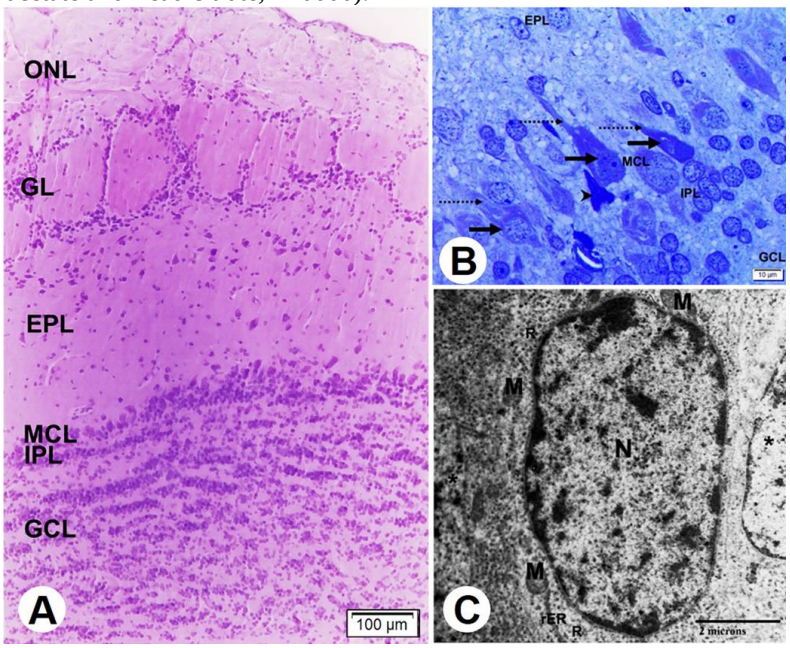

Fig. 8 [A-C]: Photomicrographs of rats' olfactory bulb sections of recovery group. **[A]:** Showing the architecture of the olfactory bulb has returned to normal with healthy appearance of the layers of the olfactory bulb, from superficial to deep: olfactory nerve layer (ONL), glomerular layer (GL), external plexiform layer (EPL), mitral cell layer (MCL), internal plexiform layer (IPL), and granular cell layer (GCL). (H&E, ×100). **[B]:** A semithin section showing the mitral cells (arrows) located in the MCL, with apical primary dendrites (dotted arrows). Some mitral cells appear small-sized and darkly stained (arrowhead) (Toluidine blue, ×1000). **[C]:** A transmission electron micrograph showing a normal mitral cell with oval euchromatic nucleus (N) and peripheral heterochromatin. The surrounding cytoplasm has many healthy organelles, mitochondria (M), free ribosomes (R) with moderate dilatation of the rough endoplasmic reticulum (rER). Parts of two adjacent mitral cells are also seen with euchromatic nuclei (*) and rich cytoplasm. (Uranyl acetate and Lead citrate, ×10000).

DISCUSSION

Tobacco smoking is one of the major causes of preventable death worldwide. The nicotine content of tobacco is responsible for many dangerous effects such as atherosclerosis, ischemic heart disease, pulmonary and renal fibrosis, and cancer (Zhang *et al.*, 2009). Ferrea and Winterer (2009) indicated that nicotine might have neuroprotective as well as neurotoxic effects expressed through complex interactions involving different neuronal circuits in humans and animals. Research studies found that olfaction is the first sensory system to differentiate during mammalian development which projects directly to the telencephalon (Shepherd *et al.*, 2021). The olfactory bulb is a neuronal center for olfaction (Fletcher *et al.*, 2009). Earlier research reported that in the presence of harmful factors, the olfactory bulb gets damaged earlier than many other parts of the brain (Velayudhan *et al.*, 2013). Thus, it can be used as an early indicator of neurodegenerative diseases and as evidence to evaluate disease progression (Velayudhan *et al.*, 2013). Patients with Alzheimer's disease show the first signs of the disease in the form of olfactory dysfunction and memory abnormalities (Velayudhan *et al.*, 2013; Misiak *et al.*, 2017). Thus, the olfactory bulb was chosen in the current research for assessing exposure to potential toxicants to the brain. However, to our knowledge, currently scarce studies are available assessing the effect of nicotine on postnatal development of the mitral cells of the olfactory bulb. Therefore, the present study aimed to clarify the consequences of nicotine injection to pregnant and lactating rats on the postnatal development of the mitral cells.

In this work, examination of the olfactory bulb in newborn nicotine-treated rats revealed profound neurodegenerative changes in the mitral cells. Many indentations of the nuclear membrane, damaged and vacuolated mitochondria, presence of lipofuscin granules, and numerous cytoplasmic vacuolations were observed in the mitral cells. Also, several vacuolations were detected in the neuropil of the olfactory nerve and external plexiform layers. It has been described that irregular nuclear shape indicates degenerative signals (Gisselsson *et al.*, 2001), premature aging, or cancer (Zink *et al.*, 2004; Scaffidi and Misteli, 2006). Commensurate with the current results, some investigators reported that nicotine has a strong affinity to the mitochondria (Cormier *et al.*, 2001; Hashimoto *et al.*, 2004). They hypothesized that altered cellular energy metabolism is involved in the pathogenesis of nicotine neurotoxicity. It was reported that the major source of lipofuscin granules is incomplete lysosomal degradation of damaged organelles (Terman *et al.*, 2006). Lipofuscin increases the cellular sensitivity to oxidative stress, as the accumulation of defective mitochondria produces more reactive oxygen species, which causes additional damage (Terman *et al.*, 2006). The presence of lipofuscin granules and mitochondrial vacuolization is associated with cell apoptosis. It was established that more lipofuscin granules indicate more autophagy in the cells (Koz *et al.*, 2012; Tripathi *et al.*, 2016). Moreover, it has been stated that cytoplasmic vacuolations usually precede cell death (Shubin *et al.*, 2016). The cytoplasmic vacuolization of mammalian cells could be transient or irreversible. The transient vacuolization was detected only during the exposure to an inducer and reversibly affect the cell (Morissette *et al.*, 2008). In contrast, irreversible vacuolization indicates cytopathological conditions leading to programmed cell death due to cytotoxic stimulus (Shubin *et al.*, 2016).

Previous investigators demonstrated that the inducers of transient vacuolization were weakly

basic amine-containing lipophilic compounds (Shubin *et al.*, 2016). At the neutral extracellular fluid, lipophilic bases were uncharged thus easily transported through the plasma membrane via the passive diffusion or active transport methods (Morissette *et al.*, 2004). When these uncharged lipophilic bases become inside the cell they pass through the organelle's membranes. However, after reaching inside the acidic endosomal-lysosomal organelles and Golgi cisterns, they become positively charged therefore losing their capacity to return to the cytoplasm. The accumulation of charged weak bases inside organelles increases the intraorganellar osmotic pressure. To equilibrate the osmotic pressure, water diffuses across the membranes of the organelles leading to the formation of the vacuoles (Aki *et al.*, 2012). A similar mechanism was suggested for the neurotoxin-induced irreversible vacuolization affecting the endoplasmic reticulum, non-acidic organelles of the endosomal-lysosomal system, and Golgi apparatus (Rogers-Cotrone *et al.*, 2010).

In the current study, the olfactory bulb of the 10-day-old treated group showed huge vacuolations in several layers. The mitral cells were damaged, having shrunken nuclei with indentation of the nuclear membrane, damaged mitochondria, lipofuscin granules and vacuolated rarified cytoplasm. These findings suggest mitral cell degeneration (Koyano *et al.*, 2005).

The present research showed alterations in the olfactory bulb of the 21-day-old treated group such as vacuolar spaces affecting several layers and engorged blood vessels of the olfactory bulb. The mitral cells were pyknotic and had cytoplasmic vacuolation, nuclear shrinkage, dilatation of the perinuclear space, lysosomal dense bodies, vacuolated swollen mitochondria, lipofuscin granules and swollen irregular axons with splitting, and irregularity of the surrounding myelin sheath. The dilatation of the perinuclear space comes in agreement with the findings of previous studies indicating necroptosis (Miyake *et al.*, 2020). Apoptosis was considered as the prototype for a regulated form of cell death; however, recent studies have established other types of regulated forms of cell death, including necroptosis (Miyake *et al.*, 2020). Dilatation of the perinuclear space in necroptosis was reported to progress through rupturing the nuclear membrane and leading to cell death. Therefore, the dilation of the perinuclear space could be considered the hallmark of necroptosis (Miyake *et al.*, 2020). The splitting and irregularity of the surrounding myelin sheath seen in the mitral cell axons could be attributed to the fact that nicotine-induced neuronal damage specifically targets the myelin sheath (Papp-Peka *et al.*, 2017). The engorged blood vessels observed in this study can be explained by other investigators that reported an increase in the olfactory bulb blood flow after nicotine injection (Uchida and Kagitani, 2020). The nicotine-induced increase in the olfactory bulb blood flow was reported to contribute to the neuronal turnover in the olfactory bulb and short-term olfactory memory thus maintaining olfactory and cognitive functions (Uchida and Kagitani, 2020).

Previous investigators have indicated that nicotine withdrawal symptoms peak on approximately the 3rd day and taper off over the course of the following 3–4 weeks (McLaughlin *et al.*, 2015). In this research, we evaluated the potential recovery from the effects of nicotine exposure in 5 weeks after nicotine withdrawal. The examination of the olfactory bulb in the recovery group of this study revealed that its architecture has returned to normal with a healthy appearance of the layers of the olfactory bulb and mitral cells. The present findings are in accordance with those of an earlier study on the effects of nicotine on the

cingulate cortex that highlighted the effects of nicotine withdrawal resulting in a marked reduction in the structural impairment of the neurons (Mahmoud *et al.*, 2013).

Nicotine at low doses has been reported to have no damaging effects on neuronal populations. However, at high doses, the neurotoxic effects are obvious (Guan *et al.*, 2003; Chambers *et al.*, 2013; Yang *et al.*, 2019). Moreover, previous research indicated that nicotine induces cellular damage both in vitro and in vivo due to the increased lipid peroxidation, creation of reactive oxygen species and oxidative stress (Kalpana *et al.*, 2004; Ayala *et al.*, 2014). Also, it induces the activity of NADPH oxidase and myeloperoxidase, superoxide mediated-DNA fragmentation, and causes malfunction of the antioxidant defense systems through the reduction of the activity of catalase and superoxide dismutase (Muthukumaran *et al.*, 2008; Mahapatra *et al.*, 2009a, b; Guo *et al.*, 2013).

The results of the present work provide evidence for the mitral neuronal degeneration induced by nicotine exposure. Upon stoppage of nicotine injections, recovery of the mitral cells occurred. However, the mechanisms underlying the cytotoxic effects of nicotine-induced mitral cell damage require further investigation.

Conclusions

Nicotine induced marked neurodegenerative changes in the mitral cells of olfactory bulbs in newborn, 10-day-old, and 21-day-old rats. The effects of nicotine appear to be reversible. Recovery occurred in 5 weeks following the withdrawal of nicotine injections, with the return to normal healthy appearance of the mitral cells as evidenced by light and transmission electron microscopy. Therefore, we encourage and advise tobacco smokers to quit smoking since recovery is promising to return to the normal healthy neuronal structure of the olfactory bulbs.

Conflict of Interest: There is no conflict of interest.

Ethics Approval: The experiments were approved by the Institutional Board Review and Ethics Committee of the Faculty of Medicine, Assiut University.

Financial Support and Sponsorship: Nil.

REFERENCES

Aki T, Nara A, Uemura K. (2012). Cytoplasmic vacuolization during exposure to drugs and other substances. *Cell Biology and Toxicology*, 28(3):125-131.

Ayala A, Muñoz MF, Argüelles S. (2014). Lipid Peroxidation: Production, Metabolism, and Signaling Mechanisms of Malondialdehyde and 4-Hydroxy-2-Nonenal. *Oxidative Medicine and Cellular Longevity*, 2014:360438.

Chambers RP, Call GB, Meyer D, Smith J, Techau JA, Pearman K, Buhlman LM. (2013). Nicotine increases lifespan and rescues olfactory and motor deficits in a Drosophila model of Parkinson's disease. *Behavioural Brain Research,* 253:95-102.

Chen WJA, Edwards RB, Romero RD, Parnell SE, Monk RJ. (2003). Long-term nicotine exposure reduces Purkinje cell number in the adult rat cerebellar vermis. *Neurotoxicology and Teratology*, 25(3):329–334.

Cormier A, Morin C, Zini R, Tillement J-P, Lagrue G. (2001). In vitro effects of nicotine on mitochondrial respiration and superoxide anion generation. *Brain Research*, 900(1):72–79.

Durante MA, Kurtenbach S, Sargi ZB, Harbour JW, Choi R, Kurtenbach S, *et al.* (2020). Single-cell analysis of olfactory neurogenesis and differentiation in adult humans. *Nature Neuroscience,* 23(3):323–326.

Ferrea S, Winterer G. (2009). Neuroprotective and neurotoxic effects of nicotine. *Pharmacopsychiatry*, 42(6):255-265.

Fletcher ML, Masurkar AV, Xing J, Imamura F, Xiong W, Nagayama S, *et al.* (2009). Optical imaging of postsynaptic odor representation in the glomerular layer of the mouse olfactory bulb. *Journal of Neurophysiology*, 102:817–830.

Fowler CD, Arends MA, Kenny PJ. (2008). Subtypes of nicotinic acetylcholine receptors in nicotine reward, dependence, and withdrawal: evidence from genetically modified mice. *Behavioural Pharmacology*, 19:461–484.

Fowler CD, Turner JR, Damaj MI. (2020). Molecular Mechanisms Associated with Nicotine Pharmacology and Dependence. *Handbook of Experimental Pharmacology*, 258:373-393.

Gisselsson D, Björk J, Höglund M, Mertens F, Cin PD, Åkerman M, *et al.* (2001). Abnormal nuclear shape in solid tumors reflects mitotic instability. *The American Journal of Pathology*, 158(1):199–206.

Guan ZZ, Yu WF, Nordberg A. (2003). Dual effects of nicotine on oxidative stress and neuroprotection in PC12 cells. *Neurochemistry International*, 43(3):243–249.

Guo C, Sun L, Chen X, Zhang D. (2013). Oxidative stress, mitochondrial damage and neurodegenerative diseases. *Neural Regeneration Research*, 8(21):2003–2014.

Hashimoto T, Yoneda M, Shimada T, Kurosawa M, Terano A. (2004). Intraportal nicotine infusion in rats decreases hepatic blood flow through endothelin-1 and both endothelin A and endothelin B receptors. *Toxicology and Applied Pharmacology*, 196(1):1–10.

Imamura F, Ito A, LaFever BJ. (2020). Subpopulations of Projection Neurons in the Olfactory Bulb. *Frontiers in Neural Circuits*, 14:561822.

Iwamoto K, Mata D, Linn DM, Linn CL. (2013). Neuroprotection of rat retinal ganglion cells mediated through alpha7 nicotinic acetylcholine receptors. *Neuroscience*, 237: 184-198.

Kalpana C, Menon VP. (2004). Protective effect of curcumin on circulatory lipid peroxidation and antioxidant status during nicotine-induced toxicity. *Toxicology Mechanisms and Methods*, 14(6):339-343.

Kouremenou I, Piper M, Zalucki O. (2020). Adult Neurogenesis in the Olfactory System: Improving Performance for Difficult Discrimination Tasks? BioEssays, 42(10): e2000065.

Koyano KW, Tokuyama W, Miyashita Y. (2005). Deeply located granule cells and mitral cells undergo apoptosis after transection of the central connections of the main olfactory bulb in the adult rat. *Neuroscience*, 131(2):293-302.

Koz ST, Etem EO, Baydas G, Yuce H, Ozercan HI, Kuloglu T, *et al.* (2012). Effects ofresveratrol on blood homocysteine level, on homocysteine induced oxidative stress, apoptosis and cognitive dysfunctions in rats. *Brain Research*, 1484:29–38.

Kuo J. (2014). Electron microscopy methods and protocols. New Jersey. Springer. Science & Business Media, CH 3, pp 1-19.

Mahapatra SK, Chakraborty SP, Das S, Roy S. (2009a). Methanol extract of Ocimum gratissimum protects murine peritoneal macrophages from nicotine toxicity by decreasing free

radical generation, lipid and protein damage and enhances antioxidant protection. *Oxidative Medicine and Cellular Longevity,* 2(4):222-230.

Mahapatra SK, Das S, Bhattacharjee S, Gautam N, Majumdar S, Roy S. (2009b). In Vitro Nicotine-Induced Oxidative Stress in Mice Peritoneal Macrophages: A Dose-Dependent Approach. *Toxicology Mechanisms and Methods,* 19(2):100-108.

Mahmoud FY, Abou-Elghait AT, Abdel-Aziz HA, Mohamed HK. (2013). Effect of chronic nicotine administration on the anterior cingulate cortex (area 24a) of adult albino rats: a histological and immunohistochemical study. *The Egyptian Journal of Histology,* 36:149-163.

Matta SG, Balfour DJ, Benowitz NL, Boyd RT, Buccafusco JJ, Caggiula AR, *et al.* (2007). Guidelines on nicotine dose selection for in vivo research. *Psychopharmacology,* 190:269–319.

McLaughlin I, Dani JA, Biasi MD. (2015). Nicotine Withdrawal. The Neuropharmacology of Nicotine Dependence. *Current Topics in Behavioral Neurosciences,* 24:99-123.

Misiak M, Vergara Greeno R, Baptiste BA, Sykora P, Liu D, Cordonnier S, *et al.* (2017). DNA polymerase beta decrement triggers death of olfactory bulb cells and impairs olfaction in a mouse model of Alzheimer's disease. *Aging cell,* 16:162–172.

Miyake S, Murai S, Kakuta S, Uchiyama Y, Nakano H. (2020). Identification of the hallmarks of necroptosis and ferroptosis by transmission electron microscopy. *Biochemical and Biophysical Research Communications,* 527(3):839-844.

Morissette G, Moreau E, C-Gaudreault R, Marceau F. (2004). Massive cell vacuolization induced by organic amines such as procainamide. *The Journal of Pharmacology and Experimental Therapeutics,* 310(1):395-406.

Morissette G, Lodge R, Marceau F. (2008). Intense pseudotransport of a cationic drug mediated by vacuolar ATPase: procainamide-induced autophagic cell vacuolization. *Toxicology and Applied Pharmacology,* 228(3): 364-377.

Muthukumaran S, Sdheer AR, Menon VP, Nalini N. (2008). Protective effect of quercetin on nicotine-induced prooxidant and antioxidant imbalance and DNA damage in Wistar rats. *Toxicology,* 243(1-2):207-215.

Nemoto T, Ando H, Nagao M, Kakinuma Y, Sugihara H. (2021). Prenatal Nicotine Exposure Induces Low Birthweight and Hyperinsulinemia in Male Rats. *Frontiers in Endocrinology,* 12:694336.

Papp-Peka A, Tong M, Kril JJ, De La Monte SM, Sutherland GT. (2017). The Differential Effects of Alcohol and Nicotine-Specific Nitrosamine Ketone on White Matter Ultrastructure. *Alcohol and Alcoholism,* 52(2): 165–171.

Rose JE, Behm FM, Westman EC, Mathew RJ, London ED, Hawk TC, *et al.* (2003). PET studies of the influences of nicotine on neural systems in cigarette smokers. *The American Journal of Psychiatry,* 160:323–333.

Rogers-Cotrone T, Burgess MP, Hancock SH, Hinckley J, Lowe K, Ehrich MF, *et al.* (2010). Vacuolation of sensory ganglion neuron cytoplasm in rats with

long-term exposure to organophosphates. *Toxicologic Pathology,* 38(4):554-559.

Scaffidi P, T. Misteli T. (2006). Lamin A-dependent nuclear defects in human aging. *Science,* 312(5776):1059-1063.

Shepherd GM, Rowe TB, Greer CA. (2021). An Evolutionary Microcircuit Approach to the Neural Basis of High Dimensional Sensory Processing in Olfaction. *Frontiers in Cellular Neuroscience,* 15: 658480.

Shubin AV, Demidyuk IV, Komissarov AA, Rafieva LM, Kostrov SV. (2016). Cytoplasmic vacuolization in cell death and survival. *Oncotarget,* 7(34): 55863-55889.

Singer S, Rossi S, Verzosa S, Hashim A, Lonow R, Cooper T, *et al.* (2004). Nicotine-induced changes in neurotransmitter levels in brain areas associated with cognitive function. *Neurochemical Research,* 29: 1779–1792.

Suvarna SK, Layton C, Bancroft JD. (2019). Bancroft's theory and practice of histological techniques. 8th ed. Authors: S. Kim Suvarna, Christopher Layton and John D. Bancroft, Elsevier Ltd.

Terman A, Gustafsson B, Brunk UT. (2006). Mitochondrial damage and intralysosomal degradation in cellular aging. *Molecular Aspects of Medicine,* 27(5-6):471–482.

Tripathi M, Zhang CW, Singh BK, Sinha RA, Moe KT, DeSilva DA, *et al.* (2016). Hyperhomocysteinemia causes ER stress and impaired autophagy that is reversed by vitamin B supplementation. *Cell Death & Disease,* 7: e2513.

Uchida S, Kagitani F. (2020). Effects of nicotine on regional blood flow in the olfactory bulb in response to olfactory nerve stimulation. *The Journal of Physiological Sciences,* 70(1):30.

Valentine G, Sofuoglu M. (2018). Cognitive Effects of Nicotine: Recent Progress. *Current Neuropharmacology,* 16(4):403-414.

Velayudhan L, Pritchard M, Powell JF, Proitsi P, Lovestone S. (2013). Smell identification function as a severity and progression marker in Alzheimer's disease. *International Psychogeriatrics,* 25:1157–1166.

Wong MK, Barra NG, Alfaidy N, Hardy DB, Holloway AC. (2015). Adverse effects of perinatal nicotine exposure on reproductive outcomes. *Reproduction,* 150: R185–R193.

Yang J, Lv DJ, Li LX, Wang YL, Qi D, Chen J, *et al.* (2019). Nicotine improved the olfactory impairment in MPTP-induced mouse model of Parkinson's disease. *Neurotoxicology,* 73: 175-182.

Zhang G, Kernan KA, Thomas A, Collins S, Song Y, Li L, *et al.* (2009). A novel signaling pathway: fibroblast nicotinic receptor alpha1 binds urokinase and promotes renal fibrosis. *Journal of Biological Chemistry,* 284(42):29050–29064.

Zink D, Fischer AH, Nickerson JA. (2004). Nuclear structure in cancer cells. *Nature Reviews Cancer,* 4:677-687.

ARABIC SUMMARY

تأثير النيكوتين والإقلاع عنه على نمو الخلايا المترالية للجرذان بعد الولادة

أيمن صلاح الدين عامر، درية عبد الله محمد زغلول
قسم التشريح الآدمي وعلم الأجنة – كلية الطب –جامعة أسيوط

الخلفية: تدخين السجائر هي مشكلة صحية عامة في جميع أنحاء العالم. يسبب محتوى النيكوتين في السجائر التعود عليه وإدمانه والعديد من الأمراض. وقد لوحظ تلف الخلايا العصبية البصلية الشمية في وقت مبكر من الأمراض التنكسية العصبية.
الهدف من البحث: توضيح تأثيرات إعطاء النيكوتين على بنية الخلايا المترالية للبصيلات الشمية في الفئران النامية، وكذلك نتائج الإقلاع عن النيكوتين.
المواد والطرق المستخدمة: تم تقسيم 24 فأر حامل بشكل عشوائي إلى مجموعتين. لم تتلق المجموعة الضابطة أي علاج، وتلقيت المجموعة المعالجة النيكوتين 6 مجم / كجم وزن الجسم/ يوم تحت الجلد يوميًا من اليوم الثامن للحمل حتى اليوم الواحد والعشرون ما بعد الولادة. تضمنت هذه الدراسة ستة ذكور من نسل الفئران في كل مجموعة في الأعمار حديثي الولادة، 10 أيام ، 21 يومًا ، وشهرين. في اليوم الواحد والعشرون ما بعد الولادة تم التضحية بستة ذكور من الفئران، وسُمح لستة فئران أخرى بالبقاء على قيد الحياة دون أي علاج حتى عمر شهرين وأعتبرت هذه هي المجموعة الشفائية. تم تشريح البصيلات الشمية وحفظها ومعالجتها من أجل الفحص المجهري الضوئي والإلكتروني النافذ.
النتائج: كانت البصيلات الشمية في جميع الأعمار من المجموعة المعالجة بها فجوات عصبية في عدة طبقات. كانت الخلايا المترالية تتدهور ولديها أنوية منكمشة، مع تعاريج في الأغشية النووية، وفراغات في السيتوبلازم والميتوكوندريا، مع وجود حبيبات الليبوفوسين بالمقارنة مع المجموعة الضابطة. وقد زادت التغيرات الإنحلالية العصبية مع زيادة عمر الفئران، وأظهرت إتساع المساحات حول النواة وتورم وعدم إنتظام الزوائد المحورية مع تشقق أغلفة المايلين في يوم ما بعد الولادة 21 مقارنةً بالمجموعة الضابطة. وعند الإقلاع عن النيكوتين عادت بنية البصيلات الشمية إلى سماتها الطبيعية.
الخلاصة: النيكوتين يتسبب في حدوث تغيرات إنحلالية عصبية في الخلايا المترالية. وقد تم شفاء الخلايا المترالية وإستردت مظهرها الطبيعي بعد الإقلاع عن النيكوتين.